Experimental quantum error correction with high fidelity

Jingfu Zhang,[1] Dorian Gangloff,[1,*] Osama Moussa,[1] and Raymond Laflamme[1,2]
[1]*Institute for Quantum Computing and Department of Physics, University of Waterloo, Waterloo, Ontario, Canada N2L 3G1*
[2]*Perimeter Institute for Theoretical Physics, Waterloo, Ontario, Canada N2J 2W9*
(Received 24 May 2011; published 15 September 2011)

More than ten years ago a first step toward quantum error correction (QEC) was implemented [Phys. Rev. Lett. **81**, 2152 (1998)]. The work showed there was sufficient control in nuclear magnetic resonance to implement QEC, and demonstrated that the error rate changed from ϵ to $\sim\epsilon^2$. In the current work we reproduce a similar experiment using control techniques that have been since developed, such as the pulses generated by gradient ascent pulse engineering algorithm. We show that the fidelity of the QEC gate sequence and the comparative advantage of QEC are appreciably improved. This advantage is maintained despite the errors introduced by the additional operations needed to protect the quantum states.

DOI: 10.1103/PhysRevA.84.034303 PACS number(s): 03.67.Lx

I. INTRODUCTION

Quantum computers could solve some problems faster than classical computers [1]. Performing a quantum computation relies on the ability to preserve the coherence of quantum states long enough for gates composing the algorithm to be implemented. In practice, the quantum coherence is sensitive to the uncontrolled environment and easily damaged by the interactions with the environment, a process called decoherence [2]. To protect the fragile quantum coherence needed for quantum computation, schemes of quantum error correction (QEC) and fault-tolerant quantum computation have been developed [3].

The 3-bit QEC code was implemented in a liquid-state nuclear magnetic resonance (NMR) quantum information processor in 1998 as the first experimental demonstration of QEC [4]. More recently, it has been implemented in trapped-ion and solid-state systems [5,6]. Here we report on using the gradient ascent pulse engineering (GRAPE) algorithm [7] to implement a high-fidelity version of the 3-bit QEC code for phase errors in liquid state NMR. The errors due to natural transversal relaxation are shown to be suppressed to a first order. In comparison with the work performed in 1998 [4], the pulse sequence fidelity is improved by about 20%, and the reduction of the first order in the decay of the remaining polarization after error correction is improved by a factor of $\sim$2.3. The advantage of the QEC is obtained although the extra operations for protecting the quantum states in QEC are subject to errors in implementation.

II. EXPERIMENTAL PROCEDURE AND RESULTS

In the current implementation, we use ^{13}C labeled trichloroethylene (TCE) dissolved in d-chloroform as the sample. Data were taken with a Bruker DRX 700 MHz spectrometer. The structure of the molecule and the parameters of the spin qubits are shown in Fig. 1, where we denote H as qubit 1, C_1 as qubit 2, and C_2 as qubit 3. The Hamiltonian of the three-spin system can be written as

$$H = -\pi \sum_{i=1}^{3} \nu_i Z_i + \frac{\pi}{2}[J_{12} Z_1 Z_2 + J_{13} Z_1 Z_3 + J_{23}(X_2 X_3 + Y_2 Y_3 + Z_2 Z_3)], \quad (1)$$

where X_i, Y_i, and Z_i denote the Pauli matrices with i indicating the spin location, ν_i denotes the chemical shift of spin i, and J_{ij} denotes the spin coupling between spins i and j. The two carbon spins are treated in the strongly coupled regime, because the difference in frequencies between the two carbons is not large enough for the weak-coupling approximation [8].

We exploit radio-frequency (rf) spin selection techniques to improve the linewidth, and hence the coherence, of the ensemble qubits [9,10]. The effect of pulse imperfections due to rf inhomogeneities is reduced by spatially selecting molecules from a small region in the sample through the rf power. We choose C_1 as the qubit to carry the state for encoding and the output state after decoding and error correction. The labeled pseudopure states $\mathbf{0}X\mathbf{0}$ and $\mathbf{0}Y\mathbf{0}$, used as the reference states with blank ancilla, are prepared by the circuit in Ref. [10], where the order is arranged as qubits 1 to 3 and $\mathbf{0} \equiv |0\rangle\langle 0|$. The qubit readout is performed on C_1, and the signals are normalized with respect to $\mathbf{0}X\mathbf{0}$ or $\mathbf{0}Y\mathbf{0}$, for different input states.

The quantum network used for implementing the QEC code is shown in Fig. 2(a), where ρ_{in} is chosen as X, Y, and Z, in separate sequences. We optimize the encoding operation and the decoding operation combined with the error correction as two GRAPE pulses [7] with theoretical fidelity >99.9%. To test the ability of the code to correct for the natural dephasing errors due to the transversal relaxation of the spins, the internal spin Hamiltonian (1) is refocused during the time delay implemented between the encoding and decoding processes. The refocusing pulse sequence is shown in Fig. 2(b), where the selective π pulses applied to spin H are hard rectangle pulses with a duration of 20 μs, while the π pulses applied to C_1 or C_2 are GRAPE pulses with a duration of 2 ms. Taking into account the strong coupling in the Hamiltonian (1), we choose the phases of the π pulses shown in Fig. 2(b) to obtain a fidelity $|\text{Tr}\{U_{\text{refocus}} E\}|/8 > 99.96\%$, where U_{refocus} denotes the simulated unitary implemented by the pulse sequence, and E denotes the identity operation.

*Current address: Department of Physics Massachusetts Institute of Technology, Cambridge, MA 02139.

(a)

	H	C_1	C_2
H	-4546.6		
C_1	201.4	-20529.5	
C_2	8.5	103.1	-21789.5

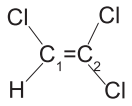

(b)

T_1(s)	8.9±0.3	8.9±0.3	13.0±0.3
T_2(s)	1.7±0.2	1.18±0.02	0.45±0.02

FIG. 1. Parameters of the spin qubits. (a) Chemical shifts shown as the diagonal terms and the couplings between spins shown as the nondiagonal terms in Hz. The inset shows the molecule structure where the three qubits are H, C_1, and C_2. (b) The relaxation times T_1 are measured by the standard inversion recovery sequence. T_2's are measured by the Hahn echo with one refocusing pulse, by ignoring the strong coupling in the Hamiltonian (1).

We choose the input states as $\rho_{\text{in}} = X$, Y, and Z, and measure the polarization that remains after error correction in ρ_{out}. The polarization ratios are denoted as f_x, f_y, and f_z. We use "entanglement fidelity," represented as

$$f = (1 + f_x + f_y + f_z)/4, \tag{2}$$

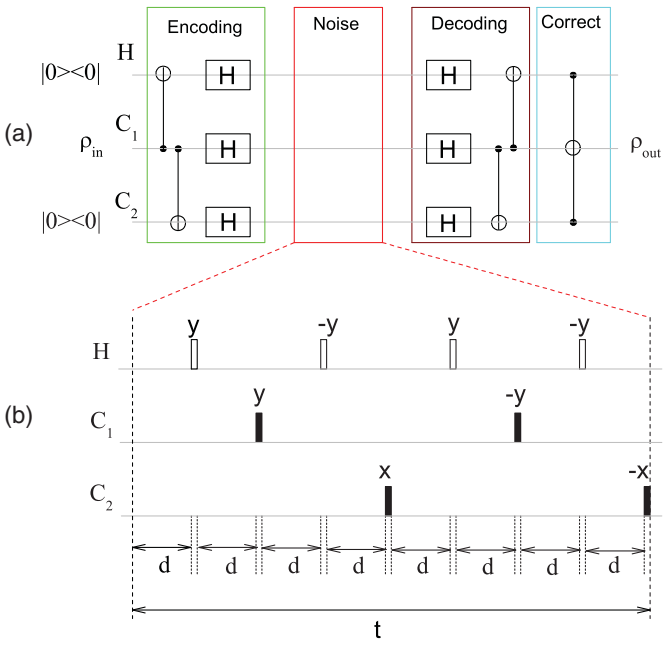

FIG. 2. (Color online) Quantum network for quantum error correction (a) where the T_2 noise is introduced by a variable time delay implemented by the pulse sequence (b) which refocuses the evolution of the Hamiltonian (1) to an identity operation with theoretical fidelity higher than 99.96%. In (b) the unfilled rectangle represents a hard π pulse with duration of 20 μs. The filled rectangle represents a GRAPE π pulse selective for C_1 or C_2 with duration of 2 ms. The phases of the pulses are denoted above the rectangles.

to characterize how well the quantum information in ρ_{in} is preserved [11].

The experimental results for QEC are shown in Fig. 3(a). For each delay time, five experiments are repeated in order to average the random experimental errors in implementation. The results of error correction (EC) are represented by •. By averaging the points for each delay time, we obtain the averaged entanglement fidelity f shown as ×, which can be fitted to $0.9828 - 0.0166t - 0.5380t^2 + 0.0014t^3$ with relative fitting error 0.73%, shown as the thick dash-dotted curve.

In order to estimate the performance of the error correction for the encoded states, we calculate the entanglement fidelity of decoding (DE) through measuring the remaining polarization before the application of the Toffoli gate, used as the error-correcting step. In this case, the decoding operation is implemented by one GRAPE pulse with theoretical fidelity >99.9%. Similar to the measurement for error correction, we also repeat five experiments for each delay time. The results are shown as ◯ in Fig. 3(a), and the data points after average are marked by +, which can be fitted as $0.9982 - 0.4361t + 0.1679t^2 + 0.2152t^3$ with relative fitting error 0.57%, shown as the thick solid curve. Here the ratio of the first-order decay terms for the two fits is found to be 26.2 ± 0.3. The important reduction of the first-order decay term indicates the high quality of state stabilization provided by QEC. As a comparison, we include the experimental data from Ref. [4], which are marked as ◇ and □ in Fig. 3(b) for the results of QEC and decoding. The data can be fitted as $0.7895 - 0.0957t - 0.0828t^2 + 0.0370t^3$ and $0.8539 - 1.1021t + 0.8696t^2 + 0.0378t^3$ with relative fitting errors 0.89% and 0.98%, respectively. The ratio of the first-order decay terms is 11.5 ± 0.2.

In implementing the QEC code, the operations associated with encoding, decoding, and error correction are subject to errors, which would lower the ability of the code to protect the quantum states. To estimate the effects of the errors, we measure the free evolution decay (FED) of ρ_{in} under the refocusing sequence shown in Fig. 2(b). Five experiments are repeated for each delay time, and the experimental data for f are shown as △ in Fig. 3(a). The averaging points, shown as ⋆, can be fitted as $1.0056 - 0.4164t + 0.3363t^2 - 0.2123t^3$ with relative fitting error 0.45%, shown as the dashed curve. The ratio of the first-order decay terms in the fits of FED and EC is 25.0 ± 0.3. Through comparing the results of QEC and FED, one can find that the errors removed by the QEC code can exceed the errors introduced by the extra operations required by the code for delay time >0.0672 s (~6% of C_1's T_2).

III. DISCUSSION

The pulse durations for encoding, decoding, and the combination of decoding and error correction are 8, 8, and 13.6 ms, respectively. We exploit the results from simulation with ideal pulses to estimate the errors due to the imperfection in pulse implementation. In simulation, we choose an uncorrelated error model for T_2 errors and ignore T_1 errors [12]. We represent the measured fidelity as $f = Af_{\text{ideal}}$, where f_{ideal} denotes the ideal fidelity by simulation and A denotes a factor to estimate the deviation between experiment and simulation. One should note that the theoretical entanglement fidelity of

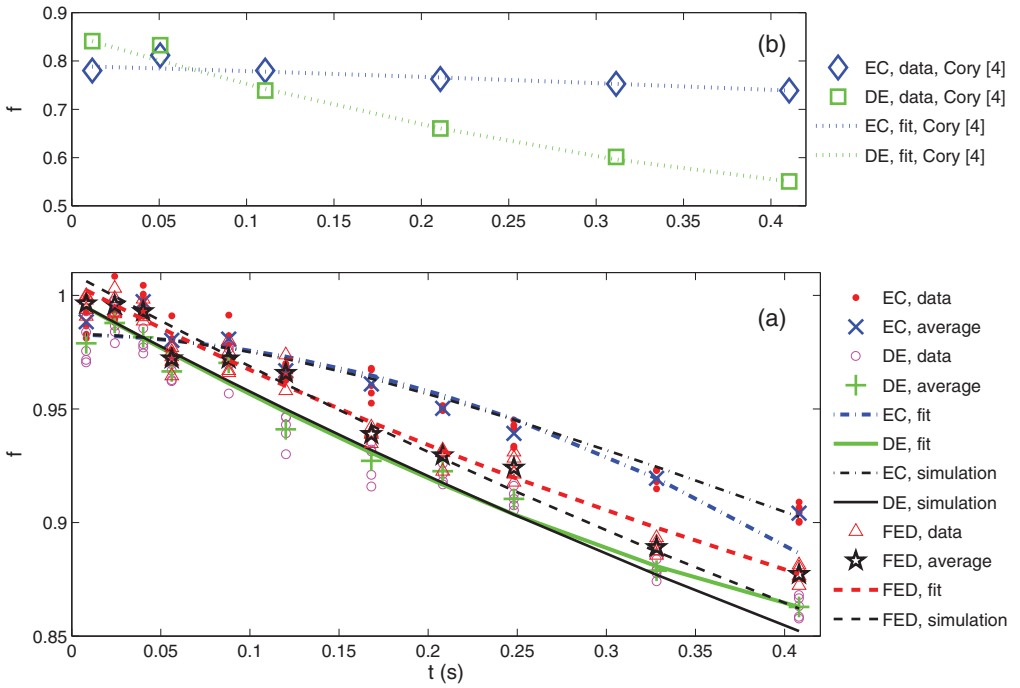

FIG. 3. (Color online) (a) Experimental results for error correction (EC), decoding (DE), and free evolution decay (FED). For each delay time, we take five data points by repeating experiments, shown as • for EC, ◯ for DE, and △ for FED. The averages are shown as ×, +, and ⋆, which can be fitted as $0.9828 - 0.0166t - 0.5380t^2 + 0.0014t^3$ with relative fitting error 0.73%, $0.9982 - 0.4361t + 0.1679t^2 + 0.2152t^3$ with relative fitting error 0.57%, and $1.0056 - 0.4164t + 0.3363t^2 - 0.2123t^3$ with relative fitting error 0.45%, shown as the thick dash-dotted, solid, and dashed curves, respectively. The ratios of the first-order decay terms in the fitted curves are calculated as 26.2 ± 0.3 for DE and EC, and 25.0 ± 0.3 for FED and EC, respectively. The thin dash-dotted, solid, and dashed curves show the fitting results using the ideal data points from simulation by introducing factors of 0.983 ± 0.006, 0.998 ± 0.007, and 1.0098 ± 0.0064 for EC, DE, and FED, respectively. (b) Results in the previous experiment [4], shown as the data marked by ⋄ and □ for EC and DE, which can be fitted as $0.7895 - 0.0957t - 0.0828t^2 + 0.0370t^3$ and $0.8539 - 1.1021t + 0.8696t^2 + 0.0378t^3$ with relative fitting errors 0.89% and 0.98%, respectively. The ratio of the first-order decay terms is 11.5 ± 0.2.

DE is the same as FED [12]. By fitting the data, we obtain $A = 0.983 \pm 0.006$, 0.998 ± 0.007, and 1.0098 ± 0.0064 for EC, DE, and FED, respectively. The fitting results are shown as the thin dash-dotted, solid, and dashed curves in Fig. 3(a). From the simulation results, we estimate the errors in implementing the operations associated with the QEC codes are about 1.2% for DE and 2.7% for EC.

IV. CONCLUSION

We optimize the encoding, decoding, and error correction as GRAPE pulses with high theoretical fidelities (>99.9%). The refocusing sequence is exploited to suspend the evolution of the Hamiltonian (1) with high fidelity (>99.96%). The quality of readout signals is further improved by rf selection. Compared with the experimental results of QEC obtained in 1998 [4], the pulse sequence fidelity is improved by about 20%. By the comparison with the free evolution decay, one can benefit from QEC even when errors exist in implementing the operations required for QEC. The improvement provided by the error correction is also demonstrated by the reduction of the first order in the decay of the remaining polarization after error correction, compared with the decay of the encoded states recovered by decoding and free evolution decay of the input states. The "QEC advantage" for the encoded states is improved by a factor of ∼2.3 from the 1998 result. In the current experiment, the second-order term in the decay after error correction is larger than the previous experiment because of the larger phase errors due to the shorter T_2 time constants [see Fig. 1(b)], noting that T_2's are 3 s for H, 1.1 s for C_1, and 0.6 s for C_2 in the previous experiment [4]. The experimental errors arise mainly from the imperfection in implementing the GRAPE pulses. Additionally, inhomogeneities of magnetic fields and the limitation of T_1 also contribute to errors.

ACKNOWLEDGMENTS

The authors acknowledge Professor D. G. Cory for helpful discussions.

[1] M. Nielsen and I. Chuang, *Quantum Computation and Quantum Information* (Cambridge University Press, Cambridge, 2000).

[2] J. Preskill, Phys. Today **52**(6), 24 (1999).

[3] E. Knill, R. Laflamme, and W. H. Zurek, Science **279**, 342 (1998); A. Yu. Kitaev, Russ. Math. Surv. **52**, 1191 (1997);

D. Aharonov and M. Ben-Or, *Proceedings of the 29th Annual ACM Symposium on Theory of Computing*, Vol. 176 (ACM Press, 1997); E. Knill, Nature (London) **434**, 39 (2005); D. Gottesman, in *Encyclopedia of Mathematical Physics*, edited by J.-P. Francoise, G. L. Naber, and S. T. Tsou (Elsevier, Oxford, 2006), p. 196.

[4] D. G. Cory *et al.*, Phys. Rev. Lett. **81**, 2152 (1998).

[5] J. Chiaverini *et al.*, Nature (London) **432**, 602 (2004).

[6] O. Moussa *et al.* (unpublished).

[7] N. Khaneja, T. Reiss, C. Kehlet, T. Schulte-Herbruggen, and S. J. Glaser, J. Magn. Reson. **172**, 296 (2005); C. A. Ryan, C. Negrevergne, M. Laforest, E. Knill, and R. Laflamme, Phys. Rev. A **78**, 012328 (2008).

[8] L. M. K. Vandersypen and I. L. Chuang, Rev. Mod. Phys. **76**, 1037 (2004).

[9] P. Maffei, K. Elbayed, J. Broundeau, and D. Canet, J. Magn. Reson. **95**, 382 (1991).

[10] E. Knill, R. Laflamme, R. Martinez, and C.-H. Tseng, Nature (London) **404**, 368 (2000).

[11] B. Schumacher, Phys. Rev. A **54**, 2614 (1996).

[12] T. F. Havel *et al.*, Appl. Algebra Eng. Commun. Comput. **10**, 339 (2000).